

Dressing of grinding wheels for the manufacture of all-ceramic micro end mills

Tobias Mayer¹, Sonja Kieren-Ehse¹, Benjamin Kirsch¹, Jan C. Aurich¹

¹TU Kaiserslautern; Institute for Manufacturing Technology and Production Systems

tobias.mayer@mv.uni-kl.de

For micro end mills, the commonly used micro end mill substrates are cemented carbides. As an alternative, all-ceramic micro end mills are recently being researched. Zirconia in particular has shown promise in achievable micro end mill geometry and cutting edge sharpness. However, the micro end mill grinding process cannot be adopted from cemented carbide. There, the grinding wheels exhibit a self-sharpening wear behavior. In contrast, grinding zirconia results in quick dulling of the grinding wheels. This in turn affects the sharpness of the manufactured all-ceramic micro end mills' cutting edges and limits the achievable structure quality in micro milling. As a result, the grinding wheels need to be trued and sharpened before/after micro end mill manufacture to achieve high cutting edge sharpness and a reproducible geometry. This study establishes a dressing setup and compares four different dressing tools. The performance is evaluated by means of the resulting grinding wheel condition. This is done qualitatively via SEM images as well as quantitatively via atomic force microscopy measurements of the micro end mills' cutting edge radii. In the experiments, pure silicon showed the best results. The dressing routine was integrated into the micro end mill production and the grinding wheel wear could largely be compensated.

Micro milling, tool grinding, ceramic micro end mills, grinding wheel dressing and sharpening

1. Introduction

Micro milling with ultra small cemented carbide micro end mills is an established micro process for prototyping needs (e.g. lab-on-a-chip systems) and small series manufacturing of individualized products such as molds and casts for micro forming processes [1]. The process is very flexible when it comes to work-piece materials and achievable geometries, in addition to being rather inexpensive for low parts volumes when compared to other micro processes such as injection molding [2]. Nearly all micro end mills are made out of cemented carbide due to its high strength and wear resistance, which is especially important for small tool diameters [3]. As an alternative, technical ceramics offer good material properties, e. g. high chemical resistance and high hardness even at elevated temperatures [4]. As such, they may allow to improve micro end mill performance by additionally utilizing their small grain sizes and their advantageous material structure. Yet, all-ceramic micro end mills are not widely used or deeply researched up to now. At our institute, all-ceramic micro end mills are being manufactured. In comparison to alumina and silicon nitride, micro end mills made from zirconia (Y-TZP) exhibited the best geometric accuracy and cutting edge sharpness after manufacturing [5], which was slightly worse than that of cemented carbide micro end mills.

However, in the initial grinding experiments without dressing, a deteriorating overall quality and sharpness of the micro end mills with the number of manufactured micro end mills became apparent. This is illustrated in Figure 1, where a new grinding wheel is compared to a used one after about 20 ground micro end mills: Looking at the circumferential surface at the top, the worn out wheel on the right has almost no protruding diamond grits left, while the initial amount of grits can be seen on the new surface of the wheel on the left. In addition to this, the corner between the radial and axial face of the grinding wheel becomes rounded and 'blurred' with increasing wear, whereas it is a clear line on the new grinding wheel. Overall, most grits have been pulled out of the binder, leading to a dull wheel and a high

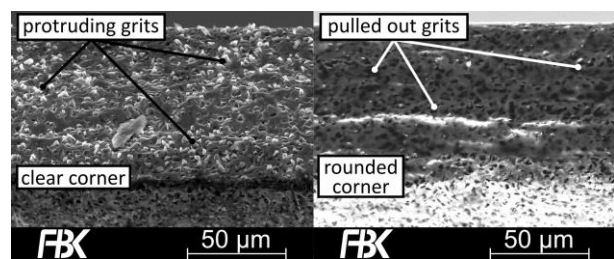


Figure 1: Comparison of a new (left) and a used (right) grinding wheel viewed at 45° (SEM images).

amount of friction. The grinding forces and the thermal loads increase, and as a result the surface quality of the micro end mills decreases. A self-sharpening behavior as observed when grinding cemented carbides is not present. As a result, the surface quality and the micro end mills' cutting edge sharpness decreases. This in turn affects the cutting process during micro milling and the achievable surface quality [6]. Increasing the diamond grit size of the grinding wheels to a large extent to reduce wear would decrease the cutting edge sharpness. As a high cutting edge sharpness is the primary objective for micro end mill production, this is not a feasible approach. Hence, there is the necessity to dress the wheels, to achieve a high cutting edge sharpness and a reproducible geometry of the micro end mills.

This study presents the modification of a grinding unit for the manufacturing of all-ceramic micro end mills to allow for dressing in between micro end mill manufacture. The wear rate of the grinding wheels is analyzed and four different dressing tools are compared in terms of their performance.

2. Experimental setup

The ceramic substrates used as micro end mill blanks ($\varnothing 3$ mm h6 x 39 mm) were made of yttria stabilized tetragonal zirconia polycrystal (zirconia/Y-TZP) supplied by Situs Technicals¹. Due to its fine grain structure and the transformation toughening mechanism, this ceramic has shown to be well suited

as base material for micro end mills. The target geometry of the tools can be achieved and sharp cutting edges can be realized via grinding [5]. To allow for the wheel dressing in this study, the existing grinding unit had to be modified. Figure 2 depicts this new setup. The grinding unit was mounted on an ultra-precision lathe LT-Ultra¹ MTC 250. Two grinding spindles equipped with diamond grinding wheels were used to manufacture micro end mills clamped in a shrink fit holder on the machine tool's spindle. The two grinding wheels were a resin-bonded wheel with grit #800 and an nickel bonded wheel with grit #4800 from DISCO HI-TEC¹. The wheel speeds were set to 10 000 rpm and 16 000 rpm, resulting in cutting speeds of 30 m/s and 46 m/s, respectively.

The coarse grinding wheel was driven by the hydrodynamic spindle of the old setup, as it was only used for bulk material removal and was not dressed. The modified unit was equipped with an NSK¹ PMS-3020K high speed spindle driving the fine grinding wheel. The PMS-3020K spindle is driven by an air turbine and features precision ground rolling bearings which can withstand higher process forces from grinding and dressing the wheel. The spindle is capable of spindle speeds up to 20 000 rpm at runouts below 1 μm . The grinding wheel was mounted on an accommodating grindstone flange. The spindle was then affixed in a split type holder to the side of the grinding unit. In addition, an industrial LEOB unit by HBM Technologie¹ was used as minimum quantity lubrication system, allowing to set a repeatable application volume of grinding fluid with a micrometre dial. As grinding fluid, Petrofer¹ ISOCOOL 600 emulsion (5 % concentration) was used. The emulsion is slightly alkaline (≈ 9.4 pH), which reduces the stress on the grinding wheels by 'softening' the ceramic material [7].

The dressing unit itself consisted of a mounting plate affixed to the right side of the spindle housing. This solution did not interfere with the micro end mill grinding process itself and was in direct proximity to the fine grinding wheel on the right side of the grinding unit. Further, no additional linear axis was needed as the machine tool's axes could be used for the dressing procedure. A piezo disc was placed on the back of the mounting plate as an acoustic emission sensor. This was used to detect the contact between the grinding wheel and the dressing tool. The voltage signal from the piezo disc was amplified with a Kemo¹ preamplifier and digitized through a National Instruments¹ USB-6210 data acquisition device. The signal was then high pass filtered (10 Hz) and displayed in LabView¹. The grinding wheel was moved to the dressing tool in 1 μm steps. Upon contact, a distinctive peak appears in the signal that can easily be identified by the operator.

As mentioned before, the machine tool's X-axis was used as

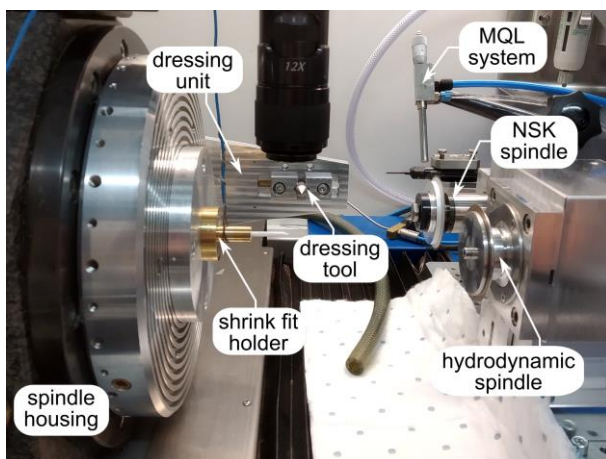


Figure 2: Modified grinding unit for all-ceramic micro end mill manufacture with wheel dressing setup.

infeed while dressing, but no additional feed movement was possible due to the axis configuration of the lathe. Also, no rotary dressing tools were used as they would need to have very low runout to not damage the grinding wheels. Such a bearing solution would have been very complex and could not have been realized within the spacial constraints. Thus, the four static dressing tools shown in Figure 3 were used: A multigrain diamond dressing tool (diamond grit size D91, dresser volume $\varnothing 4$ mm x 8 mm), a tapered single crystal diamond (scd) dressing tool (cone aperture angle 60° , tip radius 0.1 mm), a piece of pure silicon (cut from a silicon wafer to 15 mm x 15 mm) and a conventional sharpening stone (ceramic binder with grit #500 abrasives, cut to 15 mm x 45 mm). The sharpening stone and the silicon wafer pieces were placed on aluminium blocks with adhesive. These blocks were then bolted onto the mounting plate, while the two diamond dressing tools were clamped by two sliding blocks as seen in Figure 2.

For each dressing experiment, a new grinding wheel was mounted and the wheel positioning parameters were adjusted by grinding cemented carbide test cylinders and a cemented carbide micro end mill afterwards. This procedure ensures the correct micro end mill geometry after exchanging the grinding wheel. After that, three ceramic micro end mills were ground, and the grinding wheel subsequently dressed according to the experimental run. Following this, another ceramic micro end mill was ground which, in conjunction with the last micro end mill ground before dressing, was used to judge the dressing efficiency. All micro end mills were characterized via AFM after manufacture, and the grinding wheels were imaged with the SEM. The parameters of the experiments are listed in Table 1. Each dressing tool was tested with two different dressing depths. These were chosen according to the dressing tool's properties, as not to damage the thin grinding wheels. Thus, the harder scd dresser has the lowest dressing depth and the softer sharpening stone the highest. The infeed was kept constant for all dressers at 0.06 mm/min, which corresponds to the infeed of the micro end mill grinding routine.

The grinding wheels were imaged before and after dressing by scanning electron microscopy (SEM) with a FEI¹ Quanta 600 FEG. To avoid charging of the substrates, the acceleration voltage was kept at 5kV, with a working distance of 10 mm using the SE detector. Prior to SEM imaging, an ultrasonic bath with isopropyl alcohol was used to clean the substrates. The grinding wheels were imaged from an angled view at 45° looking at both the axial and radial surfaces. The micro end mills were quantitatively characterized by atomic force microscopy (AFM) using a Nanosurf¹ NaniteAFM integrated into a desktop sized machine tool.

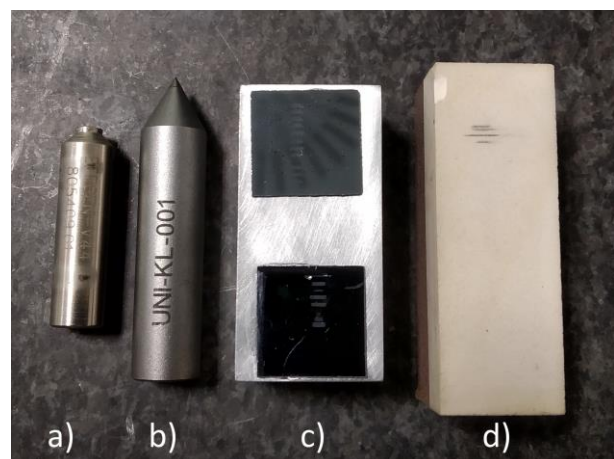


Figure 3: The four dressing tools used in this study: a) multigrain dresser, b) scd dresser, c) pure silicon and d) sharpening stone.

Table 1: Dressing depths for the different dressing tools

dressing tool	dressing depth / μm	
	low	high
scd dresser	1	3
sharpening stone	10	25
pure silicon	5	15

This allows clamping of the micro end mills in the machine tool's spindle, and positioning them angularly with a stepper motor for subsequent measurement [8]. The measurement area covered $15\ \mu\text{m} \times 8\ \mu\text{m}$, starting next to the tip of the cutting edge. Due to the high resolution of the AFM, the cutting edge geometry of the micro end mills could be accurately replicated. From the measured surface data, the overall cutting edge radius was determined using an evaluation algorithm [9].

3. Dressing experiments

To determine the necessary dressing intervals, five micro end mills were ground with one grinding wheel and characterized via AFM after manufacture. Figure 4 shows the algorithmically calculated cutting edge radius from the AFM measurements of the micro end mills and a linear fit according to [9]. The measured cutting edge radii show an increasing trend with the micro end mill count, although the second micro end mill represents an outlier. It has a higher cutting edge radius which may be due to a local defect in the ceramic micro end mill blank. Overall, an average increase in cutting edge radius after five manufactured micro end mills of about 20 % can be seen. With the above data for the grinding wheel wear and the resulting increase in cutting edge radius, a dressing interval of three micro end mills was chosen for the experiments. The increase in cutting edge radius from grinding three tools is high enough to be detected, and low enough to have a practicable number of experiments.

The multigrain diamond dresser is not included in the following results and discussion, as no ceramic micro end mills could be ground after dressing the grinding wheel with it. The micro end mills suffered such severe breakouts during grinding that the desired geometry could not be reached. Different dressing depths were tested ($1\ \mu\text{m}$, $3\ \mu\text{m}$, $5\ \mu\text{m}$) with the same result. The grinding wheel topography after dressing with the multi-grain diamond tool as examined with the SEM is shown in Figure 5, left. A very uneven topography can be identified on the circumferential surface of the grinding wheel. The top half shows heavy signs of wear with no grains protruding and a smeared section, while the bottom half remains mostly untouched aside from some smaller grooves. It seems only the top half was in contact

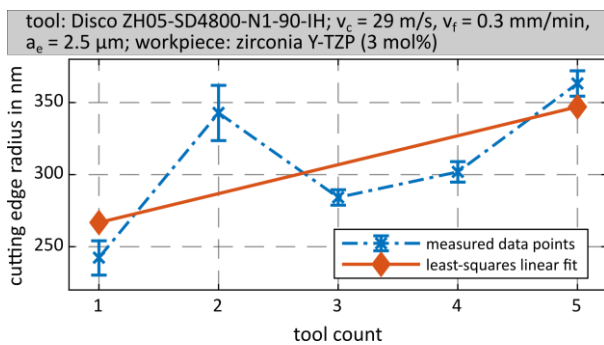


Figure 4: Cutting edge radius of ground micro end mills measured without wheel dressing versus the number ground. Displayed with 95% confidence intervals and least-squares regression fit.

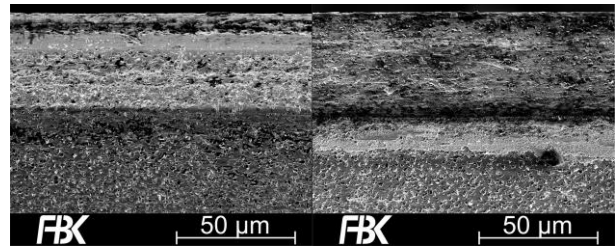


Figure 5: Grinding wheel topography after dressing with the multi-grain diamond tool (left) and the sharpening stone (right), viewed at 45° (SEM images).

with a diamond grit of the dressing tool, owing to the grain concentration of the dresser. Because the part in contact with the diamond dresser is heavily worn, it can be concluded that this dressing tool is not suitable for the intended application.

The results of the dressing runs with the other dressers are shown in Figure 6. Here, the change in cutting edge radius from the micro end mill ground before wheel dressing to the one ground after wheel dressing (i.e. the third and fourth all-ceramic micro end mill, respectively) is shown for both dressing depths tested. A negative change indicates an improvement of the cutting edge radius after dressing, i.e. a decrease, and a positive change an increase in cutting edge radius. The scd dresser leads to a large increase in cutting edge radius with the lower dressing depth, and a moderate increase for the larger one. It is possible, that the lower dressing depth leads to a wheel state where the diamond grains are still protruding from the binder to be crushed or pulled out, while the larger one also leads to removal of the binder. This could then result in more friction during grinding and thus an increase in cutting edge radius after wheel dressing for the lower dressing depth, while this not so pronounced for the higher dressing depth.

The results for dressing with the sharpening stone are reversed to the scd dresser's, with a moderate increase for the lower dressing depth and a larger increase for the higher one. A potential explanation for this behavior can be found in the adhesive layer that appears on the grinding wheel's surface after dressing. This is shown for the grinding wheel dressed with the higher dressing depth in Figure 5, right. This layer, which likely is the binder material of the sharpening stone, appears on the axial surface of the grinding wheel. It measures $25\ \mu\text{m}$ in width, which is equivalent to the dressing depth. The adhesive layer covers the grains with almost none protruding, and some burnishing can be seen around the edges towards the circumferential surface of the grinding wheel. Thus, with increasing dressing depth, the amount of adhesions increases and more friction is generated during grinding due to the covered grits. Overall, no improvement to the cutting edge radius of the ground micro end mills was made with either dressing tool for both depth settings.

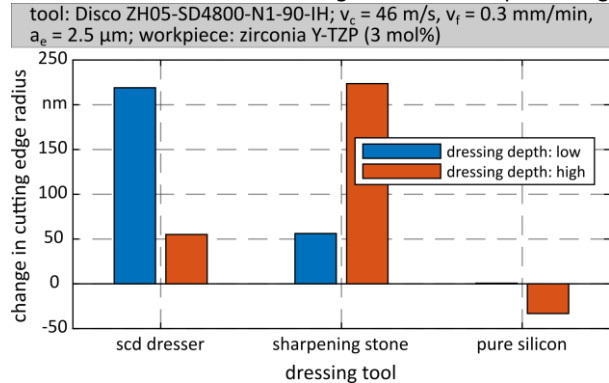


Figure 6: Change in cutting edge radius of the micro end mills after a dressing run with the different dressing tools.

Lastly, the pure silicon was able to keep the cutting edge radius level for the lower dressing depth. For the higher dressing depth, a reduction of the cutting edge radius of about $35\ \mu\text{m}$ was achieved. It appears that the material is hard enough to dress the grinding wheel unlike the sharpening stone, but soft enough not to crush the diamond grits as the scd dresser. While the reduction in cutting edge radius is not enough to return a worn grinding wheel to its initial state, it can equalize the occurring wear of each micro end mill produced. Apart from the quantitative improvement of the cutting edge radius, a slight qualitative improvement can also be seen in the cutting edge profile. Figure 7 shows the cutting edge radius profiles of the two micro end mills before and after dressing with the pure silicon. The bottom graph is more uniform, the radius is not oscillating as much and the values are more closely 'packed together'.

Overall, the pure silicon was the only dresser tested that did not worsen the grinding wheel wear, but instead resulted in an improved cutting edge radius of the manufactured micro end mill. Therefore, it was chosen as dressing tool for the all-ceramic micro end mill production for further tests. The dressing was integrated into the micro end mill production process and a dressing run performed after each end mill manufactured. To validate the findings and to test the new grinding procedure, the change in cutting edge radius of two all-ceramic micro end mills with the wheel dressed in between was measured for a total of six end mill pairs. Figure 8 shows the change in cutting edge radius measured for each micro end mill pair. The positive and negative values roughly balance each other out, and the result is a stable wear state of the grinding wheel. As such, the wheel wear could be compensated to a large extent when compared to the old grinding unit without wheel dressing in Figure 4.

4. Conclusion and outlook

In this study, the impact of grinding wheel wear on the cutting edge sharpness of all-ceramic micro end mills was determined. A dressing setup was established and four different dressing tools were tested for their ability to reduce the wear induced increase of the ground micro end mills' cutting edge radii. The

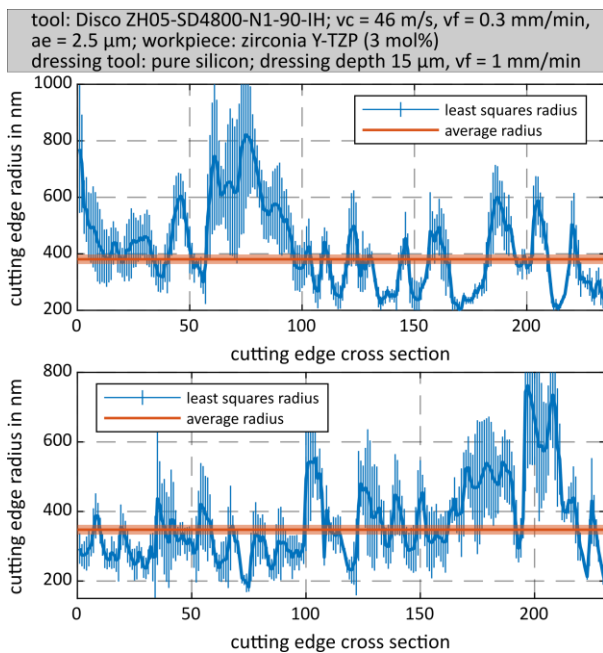


Figure 7: Calculated radii along the cutting edge of the micro end mills before (top) and after (bottom) dressing with the pure silicon. Shown with standard deviation of the individual radii and inverse-variance weighed average radius with 95% confidence interval.

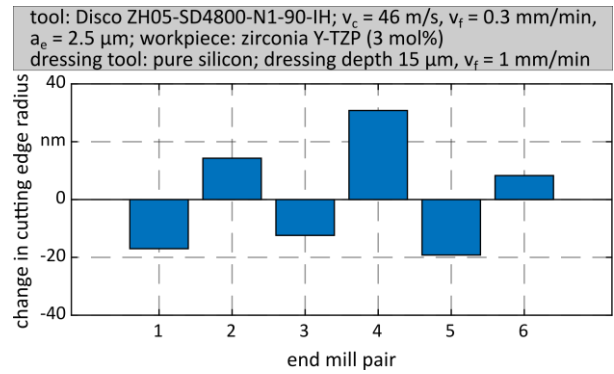


Figure 8: Change in cutting edge radius after dressing with the pure silicon for six different micro end mill pairs.

multigrain diamond dresser was not suited for this, as the grinding wheel surface was unevenly dressed and partly worn after the dressing runs. For the scd dresser and the sharpening stone the increase in cutting edge radius was dependent on the dressing depth, but no reduction could be achieved. For the pure silicon, the higher dressing depth achieved a reduction in cutting edge radius. Additionally, a slight qualitative improvement of the cutting edge profile was achieved.

With the pure silicon, the dressing procedure was integrated into the micro end mill production and the change in cutting edge radius before and after dressing monitored over six pairs of ground micro end mills. No overall increase was evident, thus the impact of grinding wheel wear on cutting edge radius could be largely compensated. In future studies, this will be monitored for a larger number of micro end mills and investigated whether multiple dressing runs can further improve the results.

Acknowledgements

Funded by the Deutsche Forschungsgemeinschaft (DFG, German Research Foundation) - project number 407558930 - associated project SFB926.

¹ "Naming of specific manufacturers is done solely for the sake of completeness and does not imply an endorsement of the named companies nor that the products are necessarily the best for the purpose."

References

- [1] Brinksmeier E, Gläbe R, Riemer O and Twardy S 2008 Potentials of precision machining processes for the manufacture of micro forming molds *Microsystem Technologies* 14 1983–7
- [2] Thepsonthi T. 2014 Modeling and Optimization of Micro-End Milling Process for Micro-Manufacturing
- [3] Chae J, Park S S and Freiheit T 2006 Investigation of micro-cutting operations *International Journal of Machine Tools & Manufacture* 46 313–32
- [4] Hülsenberg D 2014 *Keramik Springer-Verlag*
- [5] Mayer T, Kieren-Ehse S, Heintz M, Kirsch B and Aurich J C 2020 Manufacture of novel all-ceramic micro end mills *Proceedings of the 20th euspen International Conference* 113–4
- [6] Dornfeld D, Min S and Takeuchi Y 2006 Recent Advances in Mechanical Micromilling *CIRP Annals* 55/2 745–68
- [7] Novak S and Kalin M 2004 The Effect of pH on the Wear of Water-Lubricated Alumina and Zirconia Ceramics *Tribology Letters* 17/4 727–32
- [8] Kieren-Ehse S, Mayer T, Kirsch B and Aurich J C 2021 Atomic force microscope for in situ micro end mill characterization - Part I: Integration into a desktop sized machine tool *Proceedings of the 21th euspen International Conference* 463–6
- [9] Mayer T, Kieren-Ehse S, Kirsch B and Aurich J C 2021 Atomic force microscope for in situ micro end mill characterization - Part II: Development of an algorithm to characterize the cutting edge radius of micro end mills *Proceedings of the 21th euspen International Conference* 493–6